Monitoring of the polarized H_2O maser emission around the massive protostars W75N(B)-VLA 1 and W75N(B)-VLA 2

Gabriele Surcis[1], Wouter H.T. Vlemmings[2], Ciriaco Goddi[1,3] and José-María Torrelles[4,5]

[1]INAF - Osservatorio Astronomico di Cagliari, Via della Scienza 5, I-09047, Selargius, Italy.
email: gabriele.surcis@inaf.it

[2]Department of Space, Earth and Environment, Chalmers University of Technology, Onsala Space Observatory, SE-439 92 Onsala, Sweden

[3]Dipartimento di Fisica, Università degli Studi di Cagliari, SP Monserrato-Sestu km 0.7, I-09042 Monserrato, Italy

[4]Institut de Ciències de l'Espai (ICE, CSIC), Can Magrans s/n, E-08193, Cerdanyola del Vallès, Barcelona, Spain

[5]Institut d'Estudis Espacials de Catalunya (IEEC), Barcelona, Spain

Abstract. Several radio sources have been detected in the high-mass star-forming region W75N(B), among them the massive young stellar objects VLA 1 and VLA 2 are of great interest. These are thought to be in different evolutionary stages. In particular, VLA 1 is at the early stage of the photoionization and it is driving a thermal radio jet, while VLA 2 is a thermal, collimated ionized wind surrounded by a dusty disk or envelope. In both sources 22 GHz H_2O masers have been detected in the past. Those around VLA 1 show a persistent linear distribution along the thermal radio jet and those around VLA 2 have instead traced the evolution from a non-collimated to a collimated outflow over a period of $\sim$20 years. The magnetic field inferred from the H_2O masers showed a rotation of its orientation according to the direction of the major-axis of the shell around VLA 2, while it is immutable around VLA 1.

We further monitored the polarized emission of the 22 GHz H_2O masers around both VLA 1 and VLA 2 over a period of six years with the European VLBI Network for a total of four epochs separated by two years from 2014 to 2020. We here present the results of our monitoring project by focusing on the evolution of the maser distribution and of the magnetic field around the two massive young stellar objects.

Keywords. Water masers, polarization, star formation, magnetic field

---

1. Introduction

W75N(B) is an active high-mass star-forming region at a distance of 1.30±0.07 kpc (Rygl *et al.* 2012), where several massive young stellar objects at different evolutionary stages have been mapped (e.g., Torrelles *et al.* 1997; Rodríguez-Kamenetzky *et al.* 2020). Among them, VLA 1 and VLA 2 are of great interest because they are separated by only $\sim 0''.8$ (~ 1000 au) and because they host H_2O masers, whose distribution is immutable in VLA 1 and very dynamic in VLA 2 (Surcis *et al.* 2014). The spectral index analysis performed in the radio wavelength indicates that VLA 1, whose radio continuum is persistently elongated northeast-southwest, is at the early stage of the photoionization and it is driving a thermal radio jet (Rodríguez-Kamenetzky *et al.* 2020). The radio

continuum emission of VLA 2 showed a morphology variation between 1996 and 2014 from a compact roundish source (≤ 160 au; Torrelles *et al.* 1997), resembling an ultra compact H II region, to an extended source that is elongated in the northeast-southwest direction ($220 \times \leq 160$ au, $PA = 65°$, Carrasco-González *et al.* 2015). The spectral index analysis indicates that VLA 2 is a thermal, collimated ionized wind surrounded by a dusty disk or envelope (Carrasco-González *et al.* 2015). VLA 2 was also suggested to be the powering source of the large-scale high-velocity CO-outflow, oriented northeast-southwest ($PA = 66°$), that was detected from W75N(B) (Shepherd *et al.* 2003). However, the main powering source of this CO-outflow still remains unknown (e.g., Qiu *et al.* 2008).

The 22 GHz H_2O masers detected around VLA 1 and VLA 2 have been widely studied and monitored both with single dishes and interferometers, revealing high-intensity variations, with extreme maser flares (up to 10^3 Jy) and important variations in the maser distribution (e.g., Lekht & Krasnov 2000; Surcis *et al.* 2014; Krasnov *et al.* 2015). Over a period of 16 years, thanks to very long baseline interferometry (VLBI) observations, it has been observed that the evolution of the H_2O masers around VLA 1 and VLA 2, despite their close separation, is completely different. While the H_2O masers around VLA 1 are always linearly distributed ($PA \approx 43°$) along the thermal radio jet, the masers around VLA 2 are instead tracing an expanding shell (Surcis *et al.* 2014) that evolved from a quasi-circular (Torrelles *et al.* 2003; Surcis *et al.* 2011) to an elliptical structure (Kim *et al.* 2013; Surcis *et al.* 2014), following the morphology change in the continuum emission observed by Carrasco-González *et al.* (2015). Therefore, in VLA 2, the H_2O masers might be tracing the passage from a non-collimated to a collimated outflow (Surcis *et al.* 2014). In addition, Surcis *et al.* (2014) also performed polarimetric studies of the 22 GHz H_2O maser emission and they found that the magnetic field around VLA 1 has not changed between 2005 and 2012 and it is always oriented along the direction of the thermal radio jet. On the other hand, the orientation of the magnetic field around VLA 2 has changed in a way that is consistent with the new direction of the major-axis of the shell-like structure that is now aligned with the thermal radio jet of VLA 1.

In order to follow the evolution of the H_2O maser distribution around VLA 2 and to monitor any variation of the magnetic field, we performed VLBI monitoring observations toward W75N(B) of the 22 GHz H_2O maser emission in full polarization mode every two years from 2014 to 2020 for a total of four epochs. The presence of the quasi-immutable H_2O maser emission around VLA 1 will be of great importance in reinforcing the findings around the more dynamic H_2O maser source VLA 2.

2. Observations

W75N(B) was observed at 22 GHz in full polarization spectral mode and phase-reference mode with several European VLBI Network† (EVN) antennas on four epochs separated by two years: 17 June 2014 (epoch 2014.46), 12 June 2016 (2016.45), 09 June 2018 (2018.44), and 25 October 2020 (2020.82). The observational and data reduction details can be found in Surcis *et al.* (2023). In this proceeding, we just mention that the data were calibrated using the Astronomical Image Processing Software package (AIPS) by following the standard calibration procedure (e.g., Surcis *et al.* 2011) and analyzed accordingly to the procedure reported in Surcis *et al.* (2011). Briefly, this consists to identify the H_2O maser features and to measure their mean linear polarization fraction (P_l), their mean linear polarization angle (χ), and their circular polarization fraction (P_V); by modeling their polarized emission with the full radiative transfer method code (FRTM code; Surcis *et al.* 2011) we estimated the intrinsic maser linewidth (ΔV_i), the

† The European VLBI Network is a joint facility of European, Chinese, South African and other radio astronomy institutes funded by their national research councils.
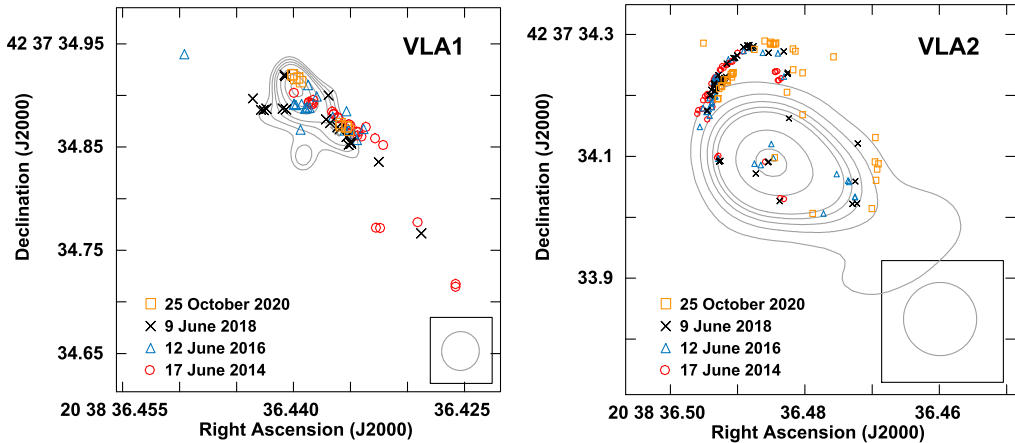
Figure 1. Comparison of the H$_2$O maser features detected toward VLA 1 (*left panel*) and VLA 2 (*right panel*) in the four EVN epochs and superimposed to the uniform-weighted continuum map at Q-band (Rodríguez-Kamenetzky *et al.* 2020) and to the natural-weighted continuum map at K-band (Carrasco-González *et al.* 2015), respectively, obtained both with the VLA. The light gray contours are 5, 6, 7, 8, 10, 12, 14 times $\sigma = 100$ μJy beam^{-1} in the case of VLA 1 and 5, 10, 15, 20, 25, 50, and 75 times $\sigma = 10$ μJybeam^{-1} in the case of VLA 2. The VLA beam is shown on the bottom right corner of both panels. The size of the symbols are ten times the uncertainties of the absolute positions of the maser features (see Table 2 of Surcis *et al.* 2023). For more details see Surcis *et al.* (2023).

emerging brightness temperature ($T_b\Delta\Omega$, where $\Delta\Omega$ is the maser beaming), the angle between the maser propagation direction and the magnetic field (θ), and the magnetic field strength along the line of sight ($B_{||}$).

3. Results

We detected H$_2$O maser features around VLA 1 and VLA 2 in all the four EVN epochs. Figure 1 shows the H$_2$Omaser features overplotted to the respective continuum emission at Q- and K-band. Here, the maser features in VLA 1 exhibit a linear distribution along the thermal radio jet but they do no show any hint of proper motions. On the other hand, the elliptical distribution of the maser features in VLA 2 suggests that the gas is not moving symmetrically around it as assumed in previous works (e.g., Surcis *et al.* 2014). Indeed, in the northeast we see that the maser features of epoch 2014.46 are generally slightly at northeast of those of the next epochs suggesting the presence of an obstacle (i.e., a denser medium) that might prevent the expansion of the gas, while we measure outward proper motions in the other directions around VLA 2. In particular, in the northwest the gas is moving outward with a velocity around 26–28 km s^{-1}; while in the center, the motion is toward southeast with a velocity around 38 km s^{-1}; in the east, the motion of the gas is toward south with a velocity of 12 km s^{-1}; in the south, the gas is expanding southward with a velocity of 8 km s^{-1}; and in the southwest the gas is the fastest one with a westward velocity of 78 km s^{-1}. These proper motions are visually reported in Figure 2. If we average the magnitude of all the velocities that we estimated, we obtain $|V| \approx 33$ km s^{-1}, similar to the symmetric expanding velocity of 30 km s^{-1} measured by Surcis *et al.* (2014).

Figure 2 shows the estimated magnetic field vectors and strengths. Here, we notice that a punctual comparison between the magnetic field vectors measured in the different epochs is more appropriate than a comparison of the averaged orientations as done previously (Surcis *et al.* 2014). Indeed, the magnetic field vectors estimated in similar
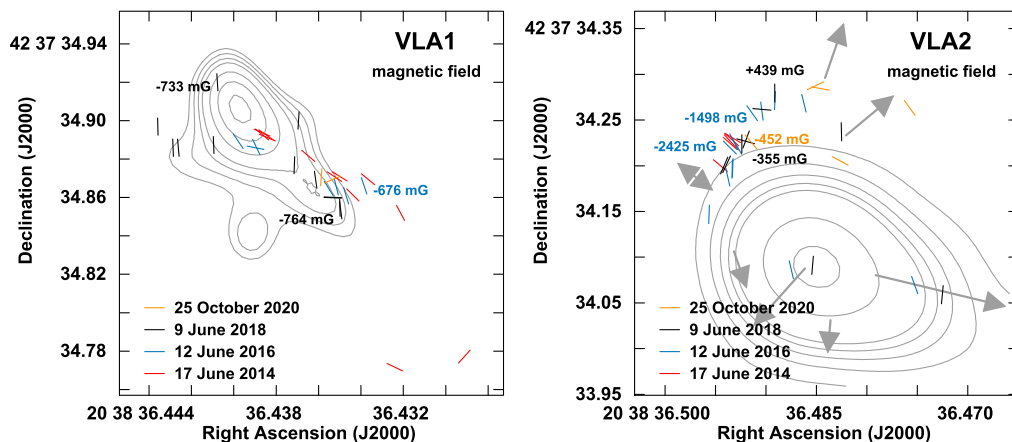
Figure 2. Magnetic field vectors and strength along the line of sight (next to the corresponding maser feature) as estimated from all the linearly and circularly polarized maser features detected around VLA 1 (*left panel*) and VLA 2 (*right panel*) during the four EVN epochs (2014.46, 2016.45, 2018.44, and 2020.82). The vectors are superimposed to the correspondig continuum map (see the caption for Figure 1). The arrows on the right panel represent the direction of the measured proper motions on the plane of the sky and their length is proportional to their magnitudes as reported in Tables 4, 5, and 6 of Surcis *et al.* (2023). The double arrow in the northeast indicates the uncertainties of the motion direction, due to the presence of an inward motion or of an outward motion of the gas.

location, but in different epochs, seem to represent a quasi-static magnetic field. We can therefore consider the magnetic field vectors estimated from the H$_2$O maser features in one epoch as representative of the magnetic field in those locations rather than just in that time. Consequently, we can gather the magnetic field vectors of all the epochs and consider them as measurements carried out at the same time. The magnetic field vectors in VLA 1 seem to follow the morphology of the continuum emission at Q-band, it is along the thermal jet and it bends toward south at the southwest end of the jet and toward north at the northeastern end. In the case of VLA 2, we found that the magnetic field is generally perpendicular to the proper motions all around the source, but in the northeast it becomes parallel after encountering the supposed denser medium. This can be explained by considering that the magnetic field component perpendicular to the shock velocity is compressed and dominate the parallel component, which remains unaffected; consequently, the resulting magnetic field is along the shock front. However, if the compression of the gas in the northeast due to the passage of the shock is inefficient, then the perpendicular component of the magnetic field is no longer able to dominate over the parallel component. The presence of the denser medium in the northeast is further suggested by the strength of the magnetic field that is higher towards northeast. A more complete analysis of the results is found in Surcis *et al.* (2023).

References

Carrasco-González, C., Torrelles, J. M., Cantó, J. *et al.* 2015, *Science*, 348, 114

Kim, J.-S., Kim, S.-W., Kurayama, T. *et al.* 2013, *ApJ*, 767, 86

Krasnov, V. V., Lekht, E. E., Rudnitskii, G. M. *et al.* 2015, *Astron. Lett.*, 41, 517

Lekht, E. E. & Krasnov 2000, *Astron. Lett.*, 26, 38

Qiu, K., Zhang, Q., Megeath, S. T. *et al.* 2008, *ApJ*, 685, 1005

Rodríguez-Kamenetzky, A., Carrasco-González, C., Torrelles, J. M. *et al.* 2020, *MNRAS*, 496, 3128

Rygl, K. L. J., Brunthaler, A., Sanna, A. *et al.* 2012, *A&A*, 539, 79

Shepherd, D. S., Testi, L., & Stark, D. P. 2003, *ApJ*, 584, 882

Surcis, G., Vlemmings, W. H. T., Curiel, S. *et al.* 2011, *A&A*, 527, A48

Surcis, G., Vlemmings, W.H.T., van Langevelde, H.J. *et al.* 2014, *A&A*, 565, L8

Surcis, G., Vlemmings, W.H.T., Goddi, C. *et al.* 2023, *A&A*, 673A, 10S

Torrelles, J.M., Gómez, J.F., Rodríguez, L.F. *et al.* 1997, *ApJ*, 489, 744

Torrelles, J. M., Patel, N. A., Anglada, G. *et al.* 2003, *ApJ*, 598, L115